CHAPTER 4

EN AW6082 METAL MATRIX COMPOSITES REINFORCED WITH MULTIWALLED CARBON NANOTUBES

Chapter – 4

EN AW6082 METAL MATRIX COMPOSITES REINFORCED WITH MULTIWALLED CARBON NANOTUBES*

The extensive review of literature carried out for the present study reveals that though a substantial amount of work has been reported on Al-based MWCNT nanocomposite, the effect on CNTs on structural, mechanical and morphological aspects of industrially important Al-alloys have not yet been investigated. In the present chapter the influence of milling time on the structure, morphology and thermal stability of multi-walled carbon nanotubes (MWCNTs) reinforced EN AW6082 aluminum alloy powders has been investigated. After structural and microstructural characterization of the mechanically milled powders micro- and nano-hardness of the composite powder particles were evaluated. Attempts have also been made to compare MWCNTs reinforced composites with that of garnet reinforced composites discussed in chapter 3.

4.1 X-ray diffraction and crystallite size

The X-ray diffraction patterns of EN AW6082-MWCNT composite powders, milled for different durations, are shown in Fig. 4.1, which shows five major peaks corresponding to FCC phase of Al. No discernible peaks for MWCNTs are observed.

* A part of this work is published in *Materials and Design* **64**, 542-549 (2014).

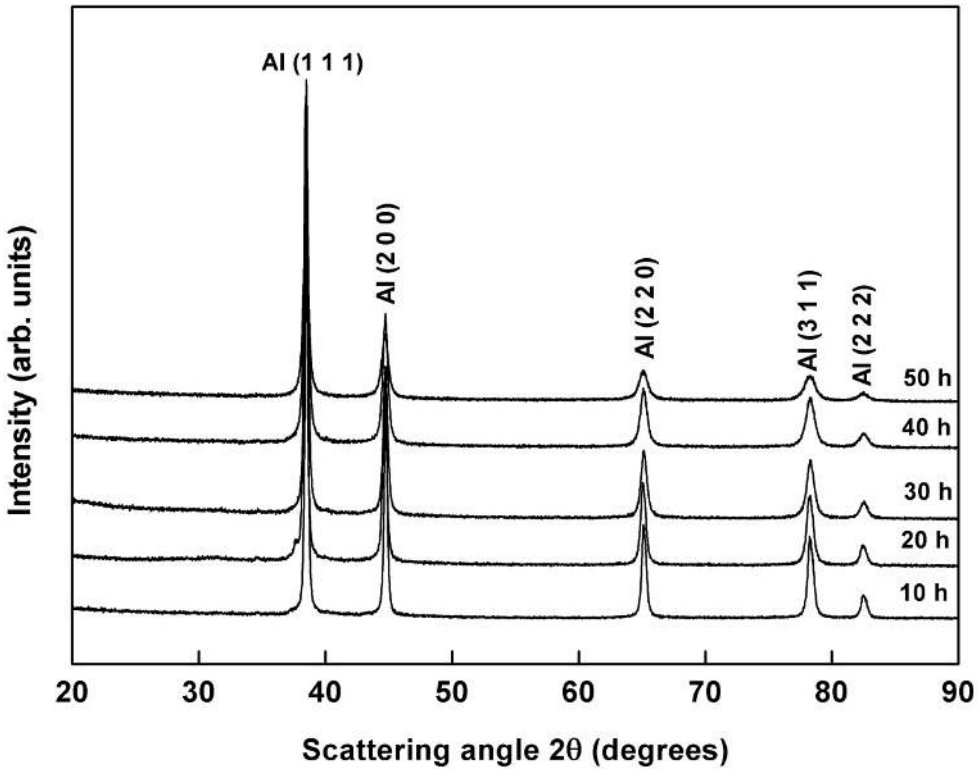

Figure 4.1: XRD patterns of EN AW6082/MWCNT powders after various milling times.

The absence of peaks related to MWCNTs and peaks corresponding to any intermetallic phase are ascribed to the small amount of MWCNTs used and the limitation of the filtered X-ray to detect phases with amount less than 2% volume fraction [Culity (2001)]. The homogenous dispersion of CNTs within the matrix, unfavorable strain conditions and amorphization of CNTs [Esawi *et al.* (2009)] could also be the reason for the absence of CNT peaks. According to the X-ray diffraction (XRD) phase analysis results, the composite consists of only Al-phase even after 50 h of milling. The width of peaks increased and their intensities became weaker as the milling time increased. This is attributed to the decrease in the crystallite size, which is due to the introduction of a large amount of defects, as the milling time increased. The

characteristic processes such as repeated deformation, cold welding and fragmentation that occur during high energy milling results in the structural changes such as crystallite size refinement, accumulation of microstrain [Tousi *et al.* (2009)] and dislocations in severely deformed powder particles. The XRD patterns recorded showed broadening and a consequent decrease in peak heights with increase in milling time. Furthermore, the diffraction lines corresponding to the aluminum were slightly shifted. The shift in position of the low angle intense peak Al (111) is shown in Fig. 4.2.

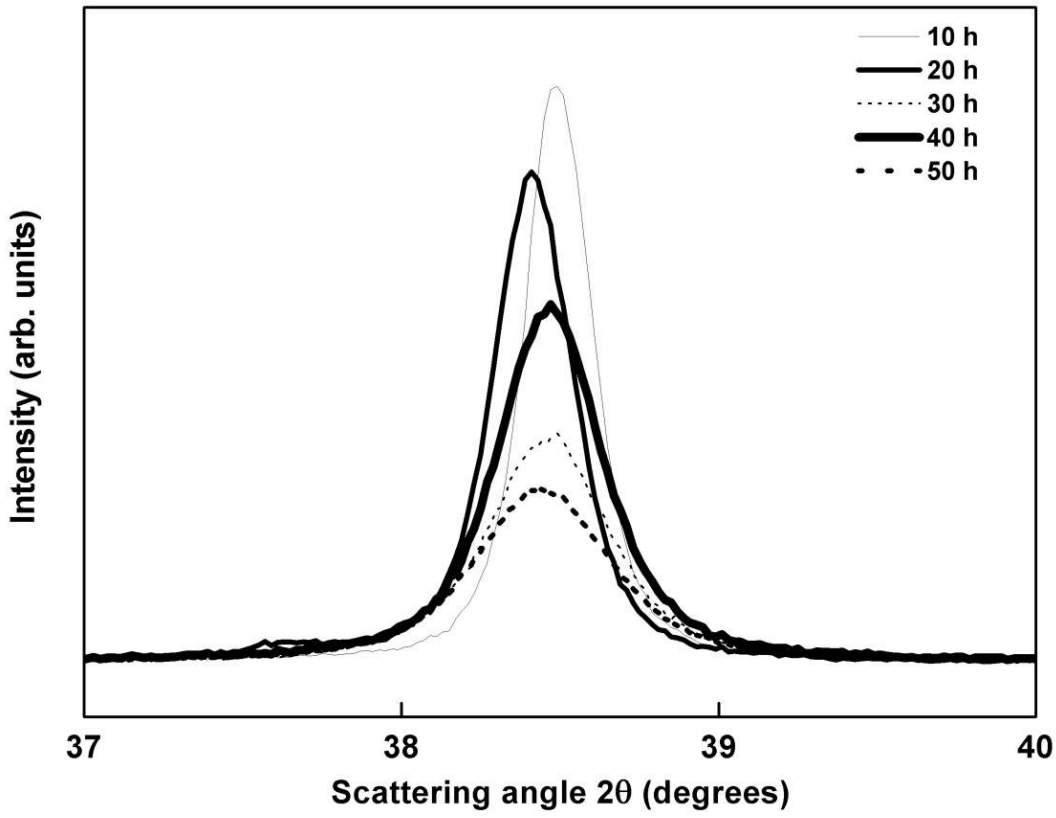

Figure 4.2: XRD pattern of first peak from the diffracting plane (111) of composite.

During initial stages of milling, a noticeable peak shift was observed towards lower diffraction angles due to the dissolution of alloying elements in the Al matrix. At the later stages of milling, no peak shifting was observed except for reduction in crystallite size, which is due to the interface structure that has a large volume fraction in nanosize materials [Dias *et al.* (1997)]. The dissolution of alloying elements, which causes displacement of diffraction peaks, is hindered at longer milling time due to uniform dispersion of MWCNTs; and hence the peak shift is minimal. It may also be possible that the large grain boundary distortion, with increasing milling time, gives way to dissolution of alloying elements in these highly energized regions that cannot be manifested in the shift of peaks due to crystalline part. It is worthwhile to note that the peak corresponding to aluminum carbide (Al_4C_3), which is often seen in the composites prepared by the liquid metallurgy route, could not be found under current milling conditions. This can be attributed to intermittent stoppage of milling process at every 20 minute interval that did not allow temperature rise for the reaction to take place. Similar findings were also reported by Esawi *et al.* (2009) in Al-CNT milled powders. The effect of milling time on the crystallite size and lattice strain for composite powders is shown in Fig. 4.3.

It is clear that the crystallite size of the composite powder decreases significantly with increasing milling time. The milled powders showed a decrease in aluminum crystallite size from around 165 nm after 10 h to about 28 nm after 50 h of milling. An increase in the lattice strain from 0.25% after 10 h to over 0.40% after 50 h of milling was observed. It is interesting to note that the crystallite size reduction was more significant in the initial stages of the milling process, i.e. up to 20 h, where the lattice strain did not increase considerably. In contrast, the lattice strain increased

significantly after 20 h of milling. The drastic reduction in the crystallite size of the Al, when milled in the presence of MWCNTs, can be partially ascribed to their hindering the movement of the dislocation by Orowan strengthening mechanism [Ruixiao Zheng *et al.* (2013)], which results in increased dislocation density and thus accelerating the grain refinement process.

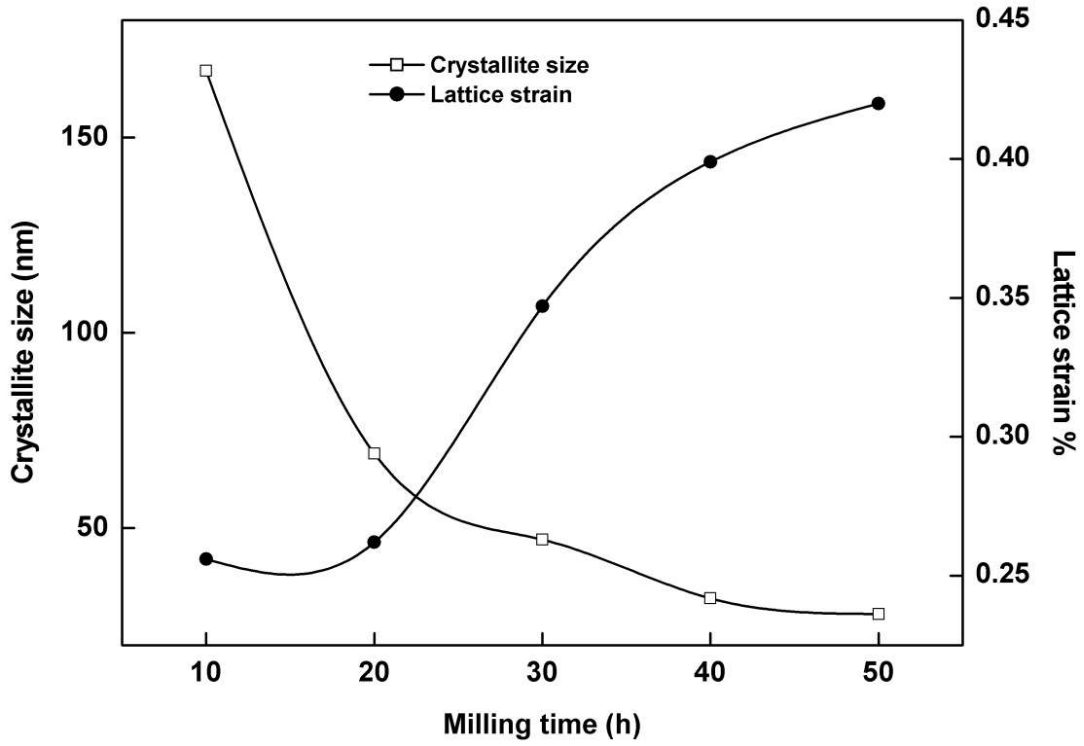

Figure 4.3: Variation in grain size and lattice strain as a function of milling time.

4.2 Particle size distribution analysis

The particle size distribution of the nano-composite powders milled for 50 h is illustrated in Fig. 4.4. It is observed that the ball milled powders possess bimodal particle size distribution. This indicates a greater tendency of CNTs to get embedded and cold welded between the soft Al matrix as a result of high energy milling. SEM

micrographs, as shown in the following section, of powders milled for 50 h further confirms the presence of bimodal particle size.

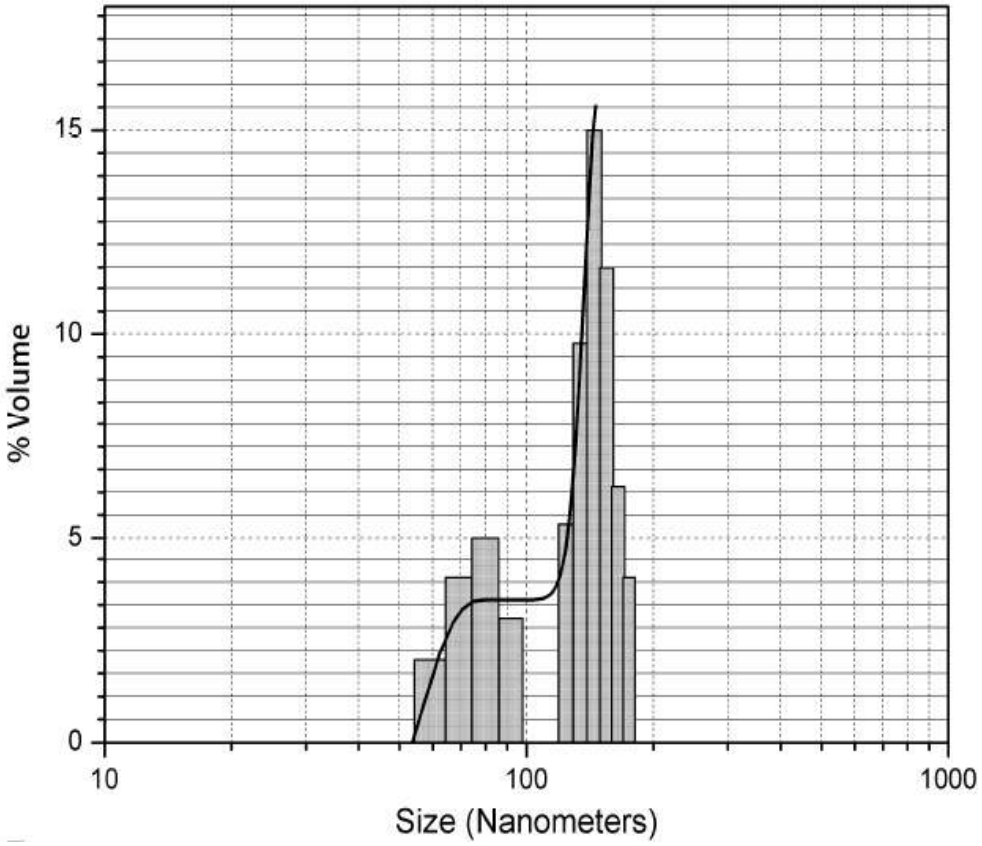

Figure 4.4: Particle size distribution of 50 h ball milled EN AW6082/MWCNT composite powder.

4.3 Morphological characteristics

The as-received EN AW6082 powder particles had an irregular spherical shape with the size distribution as shown in Fig. 4.5(a). The SEM image of the CNTs is shown in Fig. 4.5(b). It is observed that the CNTs had a curvilinear morphology and twisted shape and were having nanoscale morphological features. The morphology of powders milled for 50 h is shown in Figs. 4.5(c & d). Fig. 4.5(c) shows nearly equiaxed and refined particles indicating that the milling process has reached its steady state with

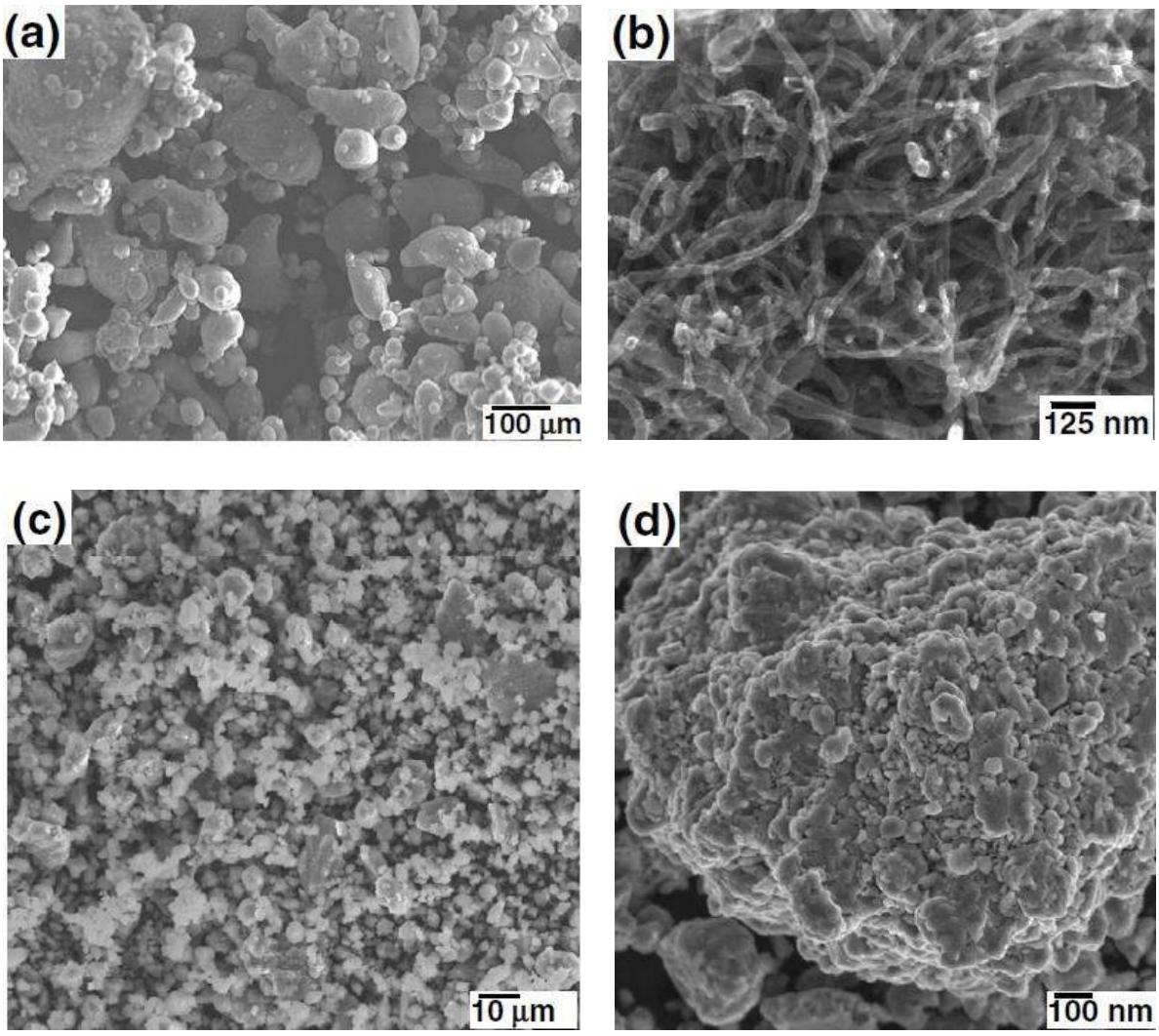

Figure 4.5: (a) The morphology of as-received Al-alloy particle (b) as-received MWCNTs (c) The morphology of EN AW6082/MWCNT composite powder after 50 h milling and (d) Magnified view of 'c'.

bi-modal particle size distribution. Fig. 4.5(d) depicts the magnified micrographs of EN AW6082/MWCNT composites milled for 50 h. It is observed that the CNT's were shortened to a large extent and got homogenously dispersed, embedded and cold welded between the soft Al matrix and tangled together as a result of high energy

milling. Similar findings were observed by Easwi *et al.* (2007) and Nayan *et al.* (2011) in their studies on the CNT-reinforced aluminum composite as a function of milling time. A significant change in matrix microstructure is expected when the reinforcement phase is in nanoscale. The lattice mismatch and difference in coefficient of thermal expansion between the matrix and reinforcement phase would lead to highly dense dislocation network, spread all around matrix-nanotube interface. It has also been reported that CNTs might act as lubricant in Al-CNT powder during the ball milling process [Kwom *et al.* (2011)]. This may affect the milling efficiency of the process.

4.3.1 TEM analysis

Fig. 4.6 shows a conventional bright field image of the 2 wt.% CNT reinforced EN AW6082 nanocomposites after 50 h of milling. The nanocrystalline structure of the milled powders and the well distributed CNTs are clearly identified. The image contrast corresponds to bent contours, grain boundaries, dislocations and CNTs dispersed into aluminum matrix. The inset image shows the corresponding selected area diffraction pattern (SADP). The ring pattern in SADP is indicative of the possibility of formation of nanostructured or fine grained composite phase. The absence of additional diffraction spots also confirms that no other phases are present. Further, no structural damage/change in the CNTs was observed under the present set of milling parameters. The MWCNTs are in the composite and are effectively embedded in the ball milled matrix powders. This effectively inhibits matrix deformation during milling and produces extensive strengthening effect [Perez-Bustamante *et al.* (2008)]. Fig. 4.7 (a) shows the high resolution transmission electron microscopy (HRTEM) image of the EN AW6082/MWCNT composite obtained after 50 h of milling. This clearly depicts that the there is some agglomeration of CNTs embedded in the matrix. Fig. 4.7(b) shows the

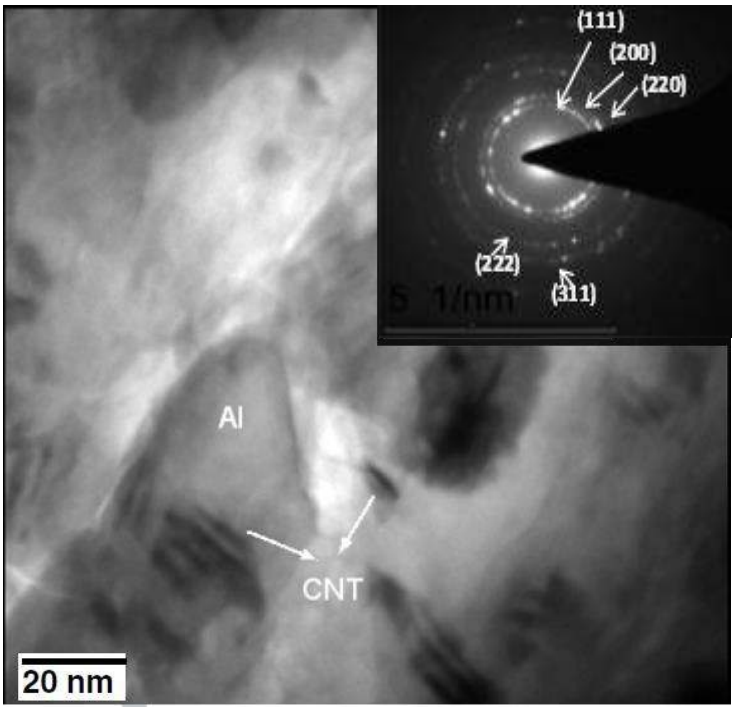

Figure 4.6: TEM bright field micrographs of 50 h MM powder particles of EN AW6082/MWCNT composite and its corresponding SAD pattern.

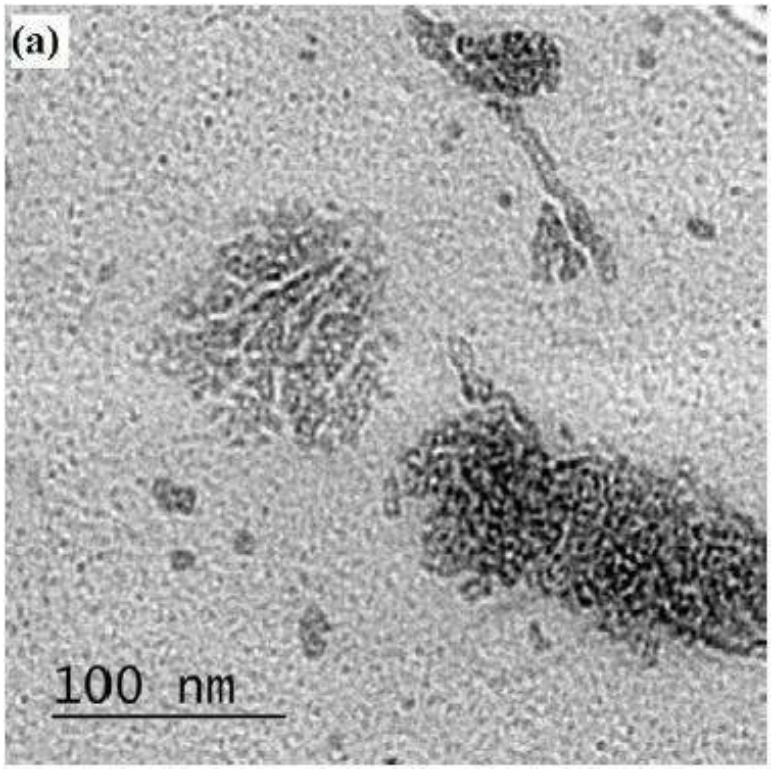

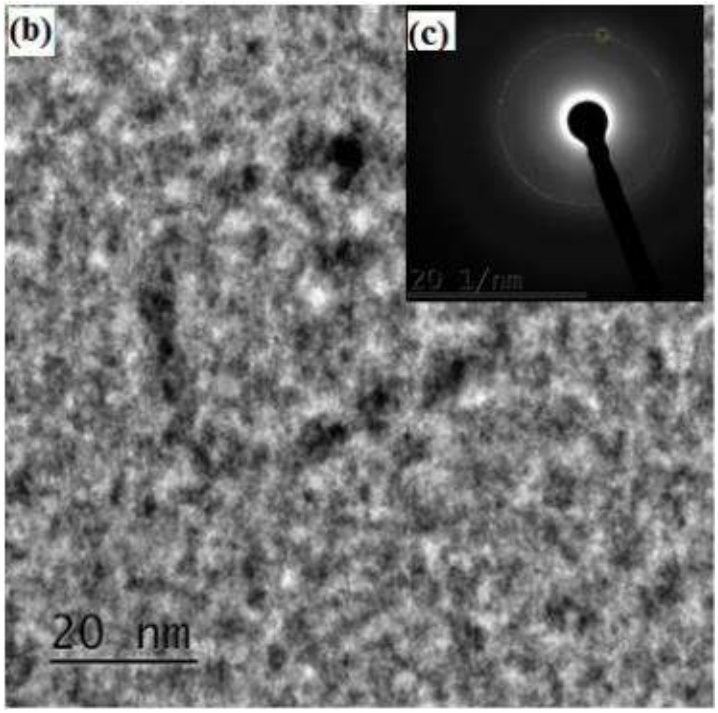

Figure 4.7: (a) HRTEM micrograph of composite powders after 50 h of the ball milling time (b) Magnified view of 'a' and (c) the corresponding SADP.

magnified image of Fig. 4.7(a) and the corresponding SADP pattern. It is evident that a prominent amount of nanocrystalline phase is present along with amorphous regions. The presence of amorphous phase could be due to adhesion of MWCNTs with the aluminum alloy matrix [Perez-Bustamante *et al.* (2010)]. The SADP pattern reveals rings arising out of the nanocrystalline regions along with the halo due to the amorphous phase pertaining to CNTs present in the matrix. Due to the detection limit of X-rays to detect phases the amorphous phase were not observed in X-ray analysis.

4.4 Thermal analysis

Fig. 4.8 illustrates the DTA analysis carried out for the powders milled for 50 h. A sharp endothermic peak at about 660^{o}C, which is attributed to the melting of aluminum alloy matrix is evident. The broad peak from 100^{o}C to 540^{o}C may be ascribed to the strain release and the grain growth as heating progresses [Dias *et al.* (1997)]. Furthermore, the small exothermic peak at about 400^{o}C to 500^{o}C was due to

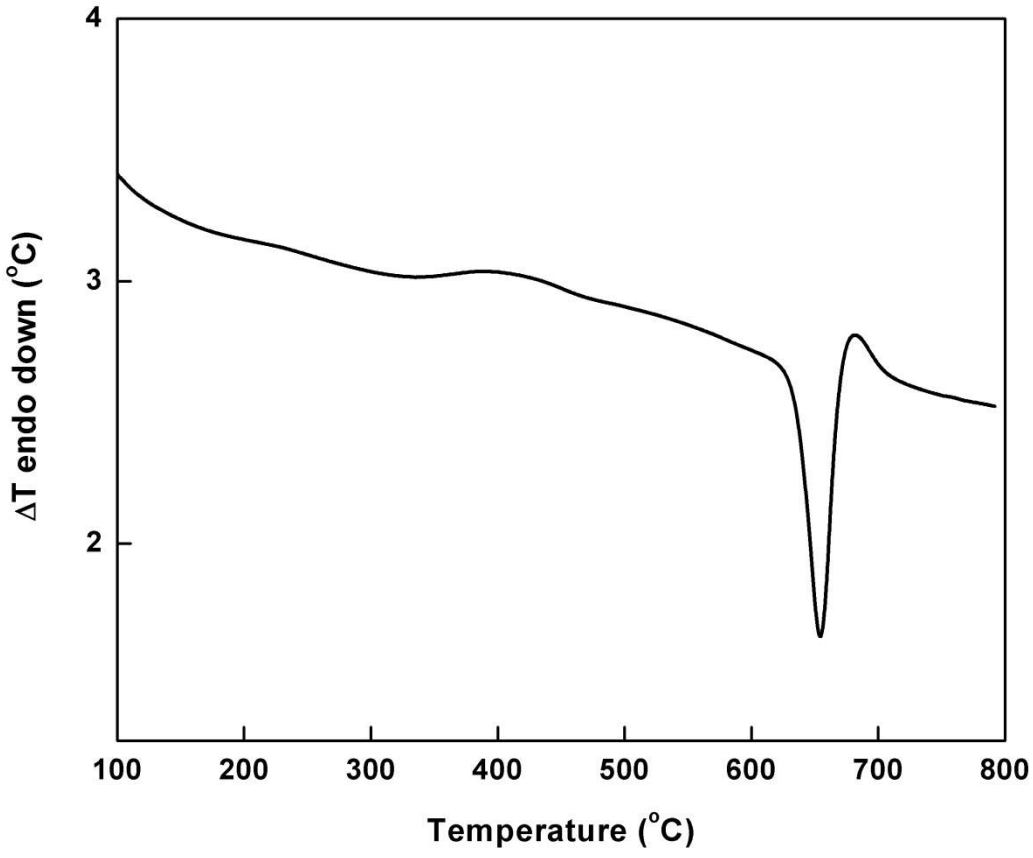

Figure 4.8: DTA scan of 50 h milled composite powder.

the dissolution of the elemental particles into the aluminum matrix as observed in unreinforced alloy. Because of the longer milling process, the diffusion couple formation, due to the dissolution of elemental powders in aluminum matrix, would lead to the release of more heat. It is therefore evident from the analysis that the milled powders could be sintered at different temperatures for consolidation, without any phase transformation. However, the effect of high temperature on the grain growth and strain release become important so far as the strengthening of the material is concerned.

4.5 Hardness evaluation

The influence of milling time on microhardness of the nanocomposite particles evaluated and is presented in Fig. 4.9. Both the unreinforced EN AW6082 and reinforced nanocomposite powder show increasing hardness values with milling time. The improved hardness in unreinforced alloy is attributed to a deformed structure produced by high energy milling. Earlier investigation by Mazilkin *et al*. (2006) has shown that solid solution hardening, increase of the dislocation density as well as the crystallite size refinement would contribute to the increase in the hardness. Generally, the mechanical properties of composites are enhanced with addition of hard reinforcement phase and with decrease in crystallite size [Gajewsla *et al.* (2014) and Varol *et al.* (2013)]. Fig. 4.9 shows that the addition of CNT to 6082 Al-alloy significantly affects the hardness. The increase in hardness for both the composite and the unreinforced alloy show a similar trend, however, with a sharp increase at the early stages of milling. The low rate of increase in hardness at longer milling time may be attributed to the completion of alloying and the occurrence of dynamic recovery due to high work hardening effect of deformed matrix.

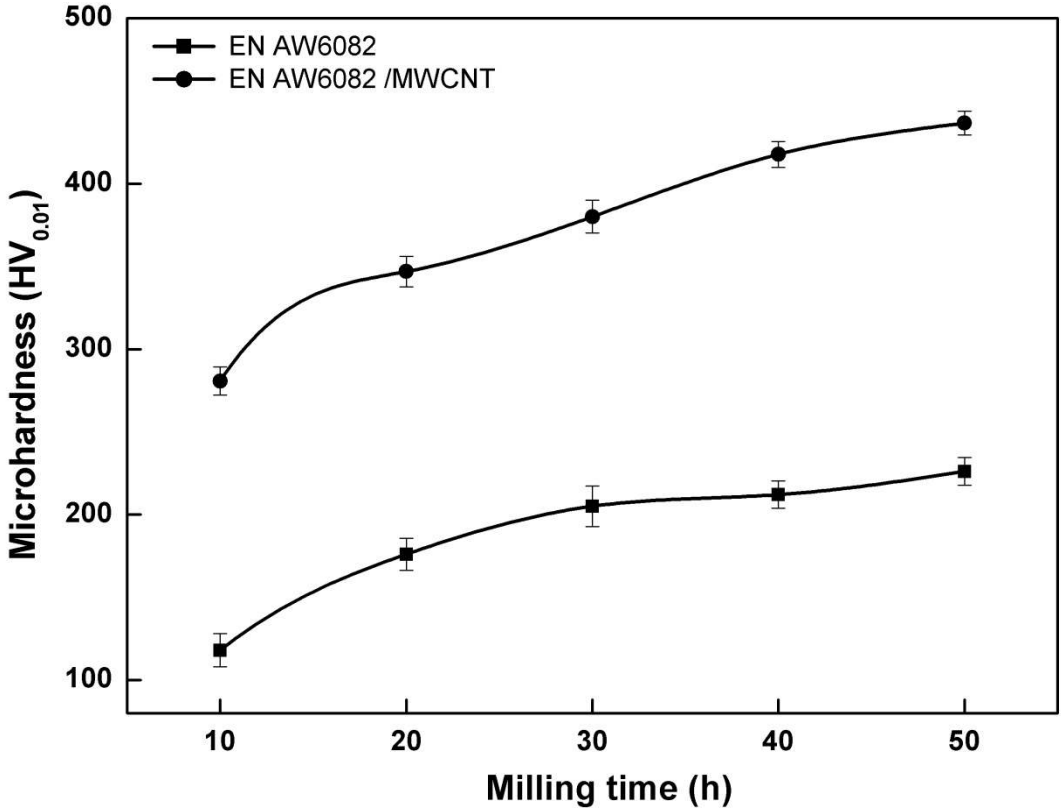

Figure 4.9: Effect of hardness of unreinforced EN AW6082 and composite powders with increasing milling time.

The addition of MWCNTs to Al-alloy accelerates the grain refinement process by the generation of high dislocation density, owing to interaction between the hard particles and dislocations. The hardness values of the nanocomposites increase with the milling time and reach a maximum value of around 436 HV after 50h of milling compared to a hardness value of less than 300 HV after 10 h of milling. These hardness values are higher than mechanically milled carbon nanotubes reinforced pure aluminum matrix composite reported by Bradbury *et al.* (2014) which revealed a maximum hardness of 151 HV with 6 wt.% MWCNTs for 20 h of milling.

The increase in hardness which is a measure of mechanical property involves combination of strengthening mechanism namely: (1) lattice strain, which increases as a result of a large amount of deformation during ball milling and introduces a high dislocation density in powder particles. The dislocation density contributes to the strength of the material and can be calculated on the basis of the Taylor equation [Ashby (1970)]; (2) interruption of dislocation movement, which can be estimated using the Orowan strengthening mechanism [Brown *et al.* (1971)]; (3) thermal mismatch between MWCNT and Al-alloy. MWCNTs have a thermal expansion coefficient of ~ 10^{-6} K^{-1} while Al-alloy have a higher value of around ~ 24 x 10^{-6} K^{-1} so consequently, the volume contraction of the Al-alloy after mechanical milling may contribute to mechanical adhesion of the MWCNTs to the matrix [George *et al.* (2005)]. The significance of this hardening mechanism will, therefore depend on the temperature rise during the milling process. However, in the present case, the temperature rise might not be very high and therefore the influence of this mechanism can be considered insignificant. Hence the strengthening due to thermal mismatch is expected to be negligible in the present experimental condition during milling. However, thermal mismatch is quite significant during processing the composites through liquid metallurgy route. Strengthening due to grain refinement can be considered important and it can be explained by well known Hall-Petch relationship.

The higher microhardness values were attained for EN AW6082/MWCNT composite powders as a result of the repeated fracturing of CNTs and its refinement. In particular, this increase in hardness is due to the presence of extremely refined hard nanoscale CNTs embedded and uniformly distributed in the Al-alloy matrix [Perez-Bustamante *et al.* (2013), Kim *et al.* (2013) and Koch *et al.* (2007)]. Perez-Bustamante

et al. (2012) and (2009) proposed that the uniform distribution of MWCNTs in the matrix effectively inhibits matrix deformation and produces a strengthening effect, resulting in an increase in mechanical properties. The other reasons which can be put forward for the increase in the composite particle hardness are (a) the work-hardening effect due to plastic deformation during milling (b) higher solubility of alloying elements in nanostructured matrix, giving rise to solution hardening [Torralba *et al.* (2003)] and (c) reduced probability of large scale of cluster formation [Torralba *et al.* (2003), Fogagnolo *et al.* (2003) and Khakbiz *et al.* (2009)].

To verify the relation between microhardness and grain size, particularly in the present case of nanoscale structures, a combination of classical Hall-Petch (H-P) equation [Hall (1951) and Petch (1953)] and Tabor relationship [Tabor (1951)], $H = 3\sigma$, is used. A linear fit of the experimental hardness values (VHN) against the inverse square root of the crystallite size ($d^{-1/2}$) results in value of H_0 and K as 10.8 ± 4 MPa and 252 ± 46 $(nm)^{1/2}$ MPa for unreinforced EN AW6082, and 19.7 ± 3 MPa and 152 ± 23 $(nm)^{1/2}$ MPa for EN AW6082/MWCNT nanocomposite, respectively. These values are higher than mechanically milled nanocrystalline pure aluminum powders reported by Abdoli *et al.* (2011) which revealed value of 7.3 ± 2 MPa and 373 ± 75 $(nm)^{1/2}MPa$ for H_0 and K, respectively, confirming that the influence of reinforcement type, size and alloying element has significant impact on the mechanical properties of the composite powders. The slope of the linear fit in both the systems is positive and, hence it can be concluded that the above relationship holds good for the

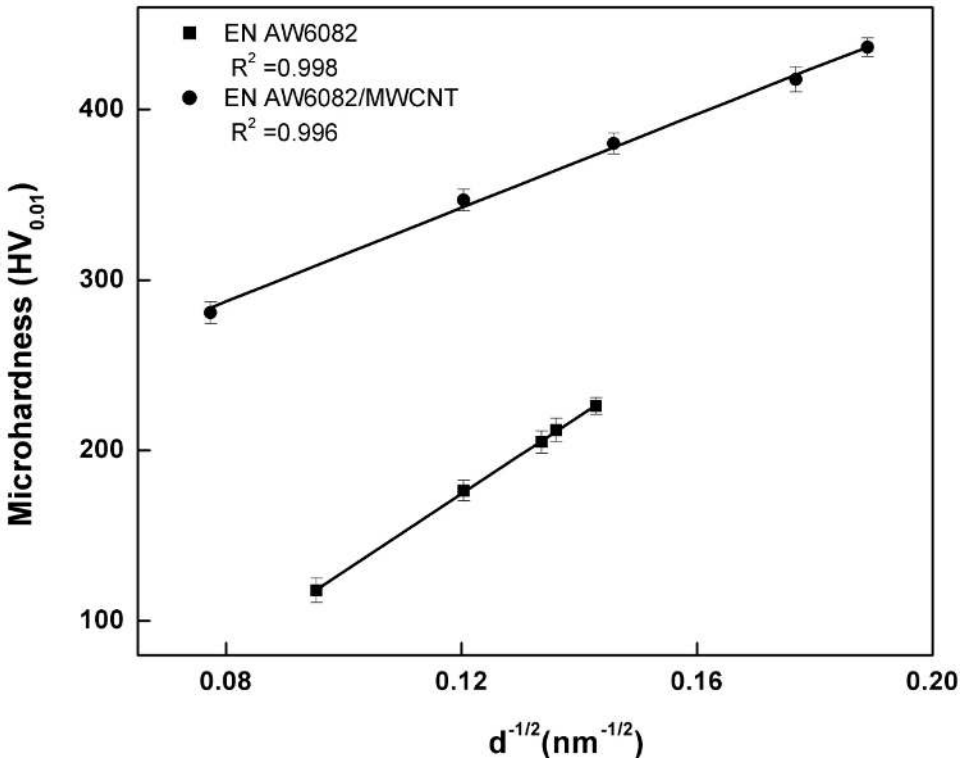

Figure 4.10: Hall-Petch effect for unreinforced alloy and composite powders compared with experimental values for crystallite size and hardness.

present investigation of nanoscale composite materials. Further, the larger slope obtained for the alloy can be attributed to high density of dislocations remaining in the milled powder [Sato *et al.* (2003)]. However, smaller slope in the case of composite indicates in-process annihilation of dislocations after reaching a saturation point. The higher lattice strain obtained for the composite may be attributed to the unsaturated CNT/matrix interfaces.

The assessment of modulus was done by using nano-indentation hardness measurement. The typical load-displacement curves for unreinforced alloy and composite powders, milled for 50 h and obtained at a peak load of 100 mN at room

temperature, is shown in Fig. 4.11. This exhibits a typical elastic behavior. The difference in the nanohardness values of the milled powders is apparent from the large differences in penetration depth. The elastic modulus and hardness, estimated from these curves, are given in Table 4.1. The nanoindendation results show that the addition of MWCNTs in EN AW6082 matrix increased the hardness and elastic modulus from 3.02 GPa and 104 GPa to 5.90 GPa and 203 GPa, respectively, after 50 h milling. With increase in milling time, the reinforcement size decreases, which has a positive effect on the mechanical properties of the composite. All nanohardness and elastic modulus values obtained are higher than that of pure aluminum, which has a hardness value of 0.7 GPa and elastic modulus of 76 GPa. A comparison of the nanoindentation and the Vickers hardness values for the alloy as well as the composite powders, milled for 50 h, is shown in Fig. 4.12. The Vickers as well as nanohardness values for the composite powders are twice the values obtained for the unreinforced alloy powder. This behavior may be attributed to the finer grain size and to the addition of nanosize CNTs to the Al-alloy matrix. Orowan strengthening, grain and substructure strengthening, quench

Table 4.1: Elastic modulus and hardness of the unreinforced alloy and EN AW6082/2 wt %MWCNT composite milled for 50 h measured by nanoindentation.

System	E (GPa)	H (GPa)
EN AW6082	104 ± 12	3.02 ± 0.4
EN AW6082/MWCNT	203 ± 7	5.90 ± 0.2

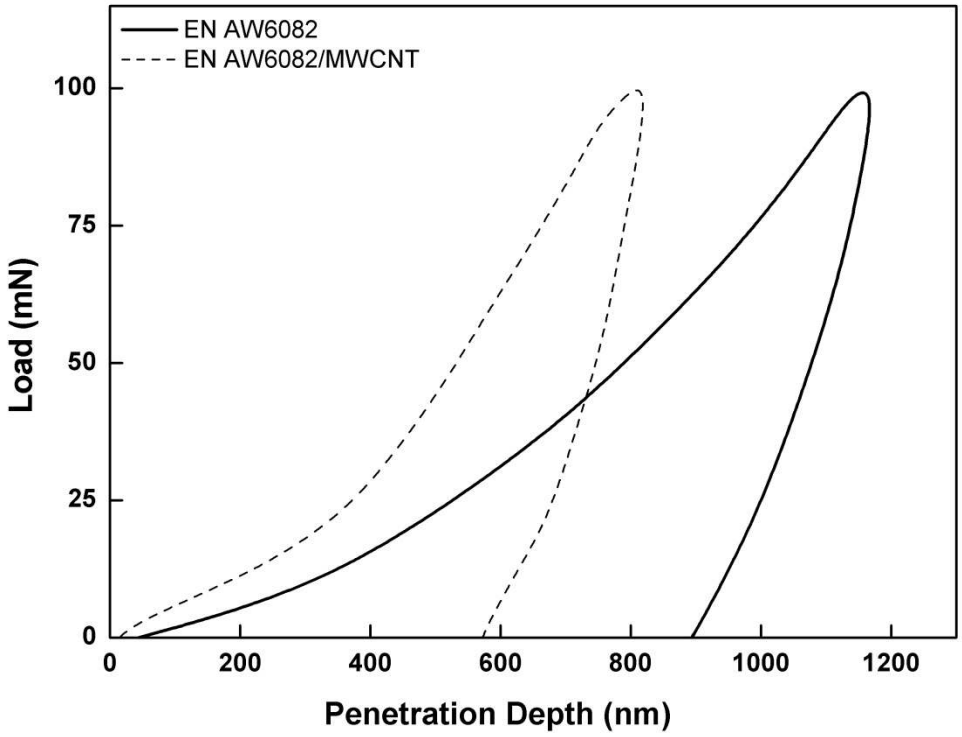

Figure 4.11: Load versus penetration depth curves of unreinforced EN AW6082 and composite powders as-milled for 50h.

hardening resulting from the dislocations generated to accommodate the differential thermal contraction between the reinforcing particles and matrix, and work hardening due to the strain misfit between the elastic reinforcing particles and the particle matrix [Lloyd (1994)] are the possible strengthening mechanisms which may operate simultaneously leading to increased hardness and elastic modulus of the particle-reinforced metal matrix composites. The indentation size effect (ISE) is generally held responsible for the difference in microhardness and nanohardness values [Mukhopadhyay *et al.* (2006)].

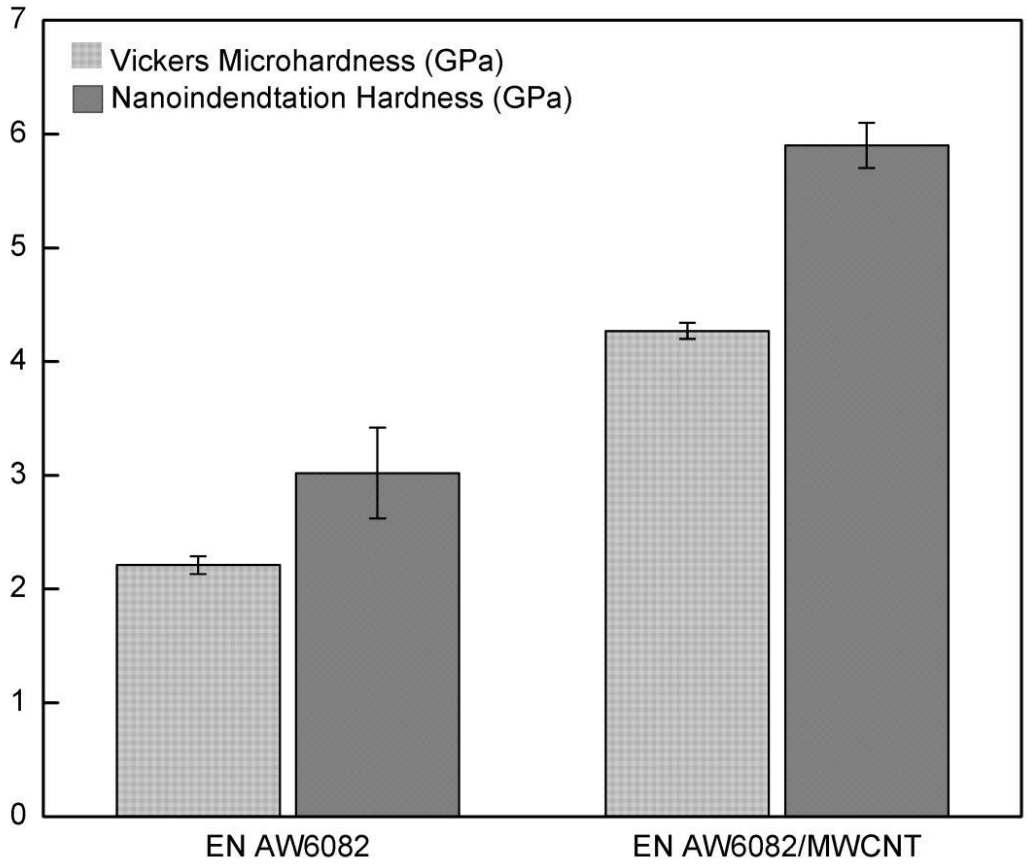

Figure 4.12: Vickers micro and nano-indentation hardness of 50 h ball milled powders.

4.6 Comparative studies on EN AW6082 composites reinforced with garnet and multi-wall carbon nanotubes

4.6.1 Structural characterization

X-ray diffraction patterns of the mechanically alloyed powders of EN AW6082/Garnet and EN AW6082/MWCNT powders are shown in Fig. 4.13. For comparison, typical XRD pattern of as-received EN AW6082 is also shown. It is noticed that for unreinforced EN AW6082, minor peaks related to major alloying

elements were visible. During milling with garnet and MWCNTs as reinforcement, peaks related to alloying elements vanished and the major peaks of aluminum were present. Further peak shift in composite powders, which is indicative of formation of supersaturated solid solution and/or dissolution of alloying elements into Al-matrix, as noticed by earlier researchers [Lu *et al.* (1997), Bathula *et al.* (2012), Sivasankaran *et al.* (201) and Daquino-Lara *et al.* (2011)] was not evidenced. This outcome clearly

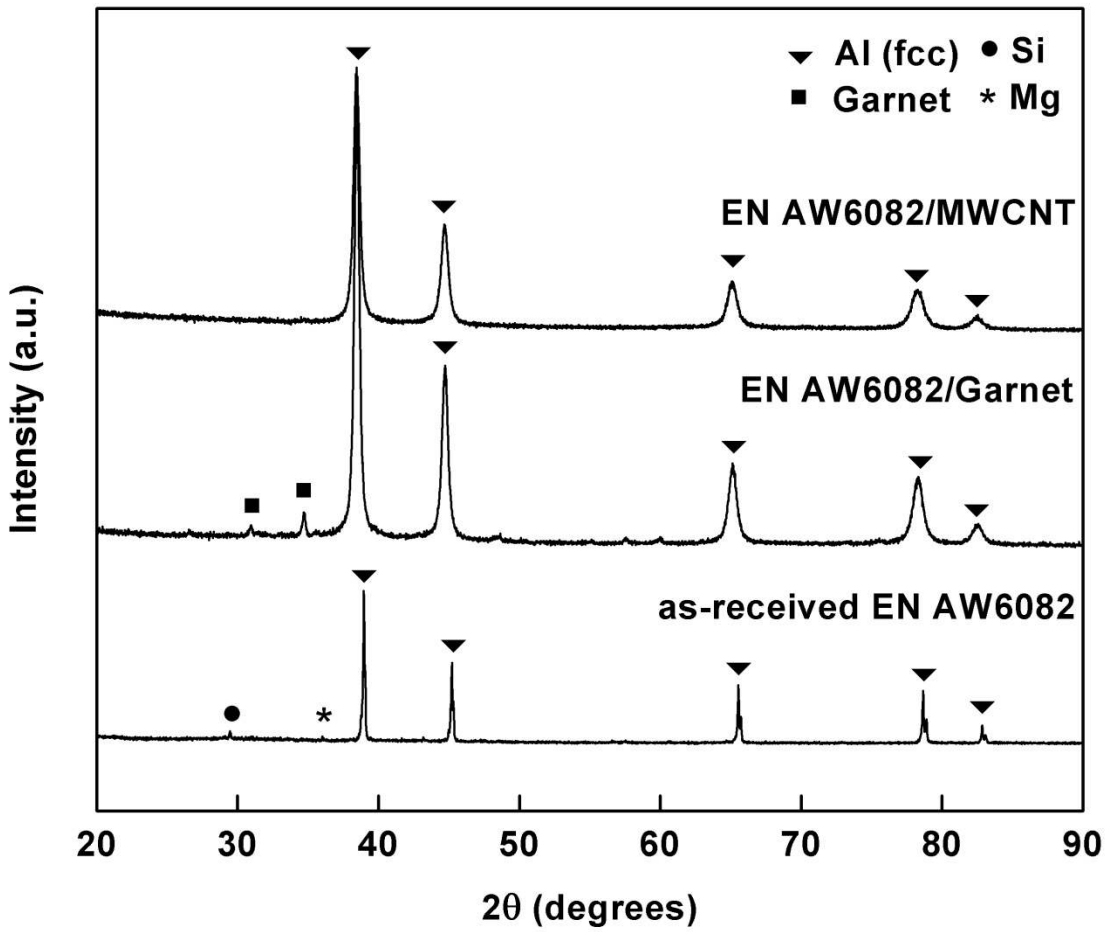

Figure 4.13: XRD patterns of as-received unreinforced EN AW6082 alloy and mechanically milled EN AW6082/Garnet and EN AW6082/MWCNT composite powders after 50 h.

indicates that the complete dissolution of alloying elements into the Al-alloy matrix has reached before milling time of 50 h and the hard rigid dispersoids got homogenously dispersed and hinders related peak shift due to increased solubility. The absence of MWCNT peak in EN AW6082/MWCNT and any intermetallic peaks in composite powders can be attributed to the limitation of the filtered X-ray to detect phases with amount less than 2 % volume fraction [Cullity (2001)]. In contrast, garnet peak was evidenced in EN AW6082/Garnet due to its higher volume fraction (5 wt. %). As an indicative of grain refinement as well as creation of lattice strain during milling considerable peak broadening was observed. A comparison of the variation in crystallite size and lattice strain with different reinforcements (Table 4.2) indicates that the high-energy ball milling and reinforcement type has a significant influence on both

Table 4.2: Mean crystallite size and lattice strain of powders milled for 50 h.

Material	Crystallite size (nm)	Lattice strain (%)
EN AW6082/Garnet	36 ± 4	0.369 ± 0.0032
EN AW6082/MWCNT	28 ± 6	0.420 ± 0.0029

grain refinement and the introduction of lattice strain. The mean crystallite size determined using Williamson-Hall plot was around 36 nm and 28 nm for garnet and MWCNT reinforced composites powders, respectively. In parallel with the strong reduction in crystallite size compared to unreinforced EN AW6082 and composite powders [Raviathul Basariya *et al.* (2015)], mechanical milling introduces a considerable amount of lattice strain. The augmented microstructural refinement down

to nanometer range, in both EN AW6082/Garnet and EN AW6082/MWCNT, is due to presence of hard abrasive garnet particles and dispersion of nanosized carbon tubes.

4.6.2 Microstructure and morphology

Figure 4.14 and 4.15 shows the bright field TEM micrograph of the garnet and CNT reinforced composite particle after 50 h of milling. As observed, there is a homogenous distribution of two different phases (dark and light) corresponding to matrix and reinforcement and the microstructure revealed the nanocrystalline nature of the composite powder. The image contrast evidenced in the micrographs corresponds to grain boundaries, dislocations, contours and dispersion of reinforcement particle into

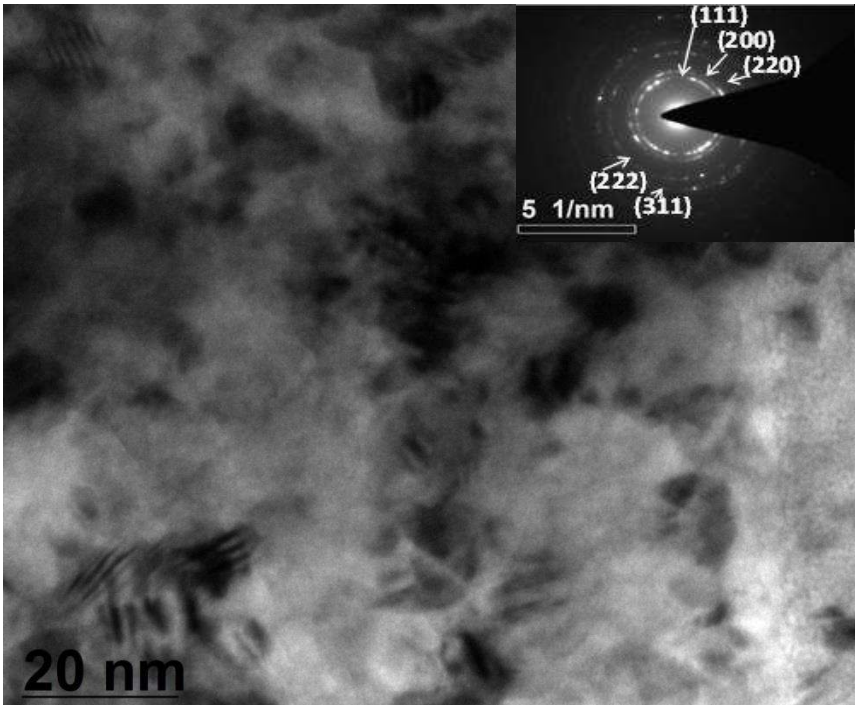

Figure 4.14: TEM bright field image of 50 h MM powder particles of EN AW6082/Garnet composite and its corresponding SAD pattern.

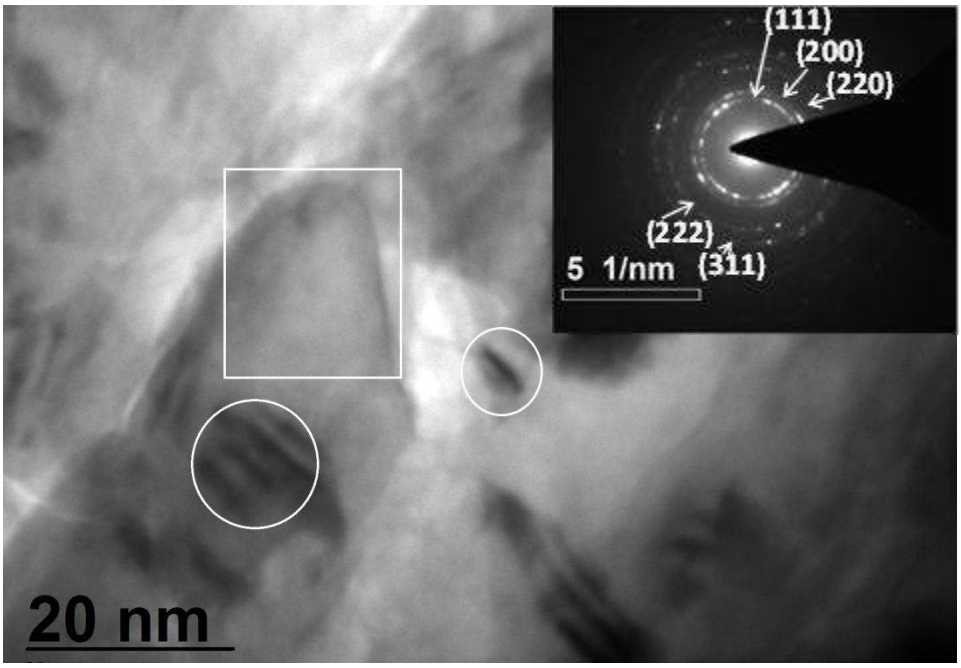

Figure 4.15: TEM bright field image of 50 h MM powder particles of EN AW6082/MWCNT composite and its corresponding SAD pattern.

aluminum matrix. The corresponding selected area diffraction pattern (SADP) indicative of the formation of nanostructured and/or fine grained composite phase is evident from inset of Fig. 4.14 and 4.15. In case of EN AW6082/MWCNT, the CNTs in the composite got effectively embedded as encircled in the equiaxed Al-alloy matrix (marked as square) as shown in Fig. 4.15. Fig. 4.16 (a-c) shows the high resolution transmission electron microscopy (HRTEM) images of mechanically milled EN AW6082/Garnet and EN AW6082/MWCNT composite powders at different magnifications after 50 h of high energy ball milling. The nanocrystalline structure of the milled powders and the well distributed reinforcement are clearly identified. For EN AW6082/Garnet the micrograph (Fig. 4.16a) clearly depicts that the abrasive garnet

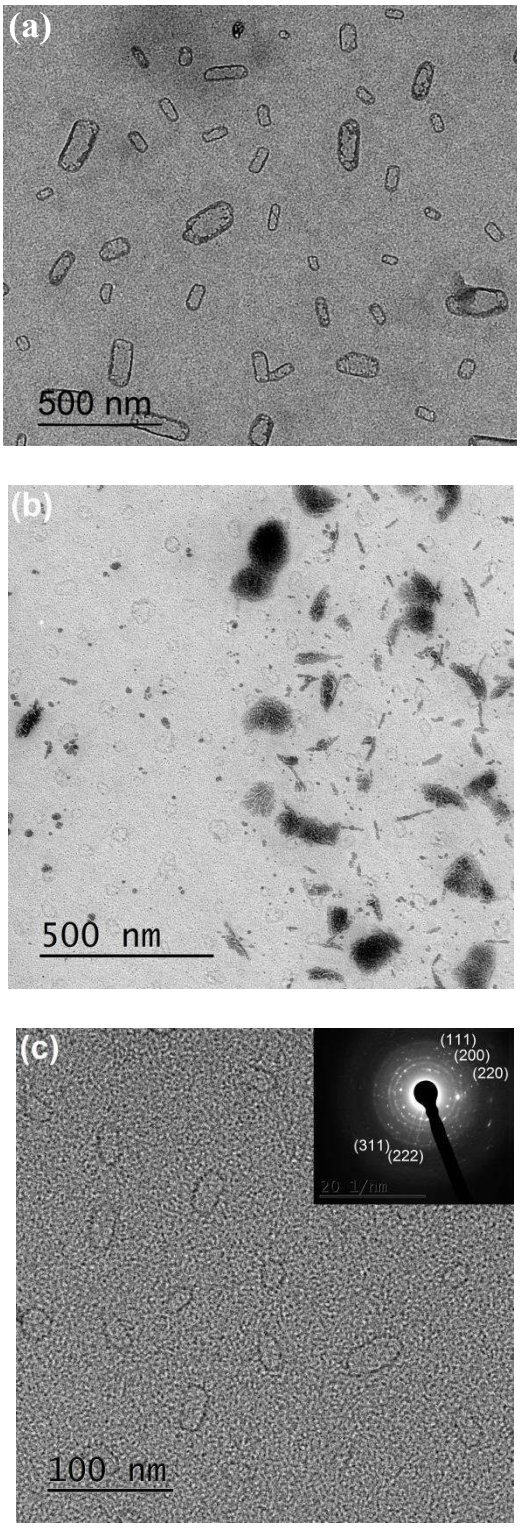

Figure 4.16: HRTEM images of EN AW6082/Garnet and EN AW6082/MWCNT composite powders at different magnifications.

particles got evenly dispersed in continuous aluminum matrix. Its higher magnification image (Fig. 4.16c) and corresponding SADP confirms crystalline nature. In case of EN AW6082/MWCNT the HRTEM image (Fig. 4.16b) depicts that the MWCNTs were densely packed by Al-matrix without any structural damage. Further, some agglomeration of CNTs embedded in the matrix was revealed. It is evident from the micrographs that a prominent amount of nanocrystalline phase is present along with amorphous regions. The existence of amorphous phase can be attributed to the adhesion of hard reinforcements with the aluminum alloy matrix [Suryanarayana (2001)]. Microstructural characterization confirms that no intermetallic compound/layer was formed at the interface of aluminum matrix and reinforcement and the results are in agreement with structural characteristics obtained using XRD.

4.6.3 Hardness variations

Figure 4.17 compares the Vickers microhardness of EN AW6082/Garnet and EN AW6082/MWCNTs composite powders. The hardness value of the MWCNT reinforced composites is higher than that of the garnet reinforced powders. These results indicate that the MM process is beneficial and the selected conditions for the MM process in the current research were optimal for the reinforcements used. The hardness values of 313 HV and 436 HV were achieved for the EN AW6082/Garnet and EN AW6082/MWCNTs composite powders, respectively. The addition of garnet and MWCNTs to Al-alloy accelerates the grain refinement process. However, the hardness in case of reinforcement with MWCNTs, which has both ductile and brittle nature, can be due to competing effects of both ductile-brittle and ductile-ductile mechanism of MA/MM which leads to increased dislocation density within the matrix. On the other hand, the addition of MWCNTs to an aluminum matrix can easily improve the modulus

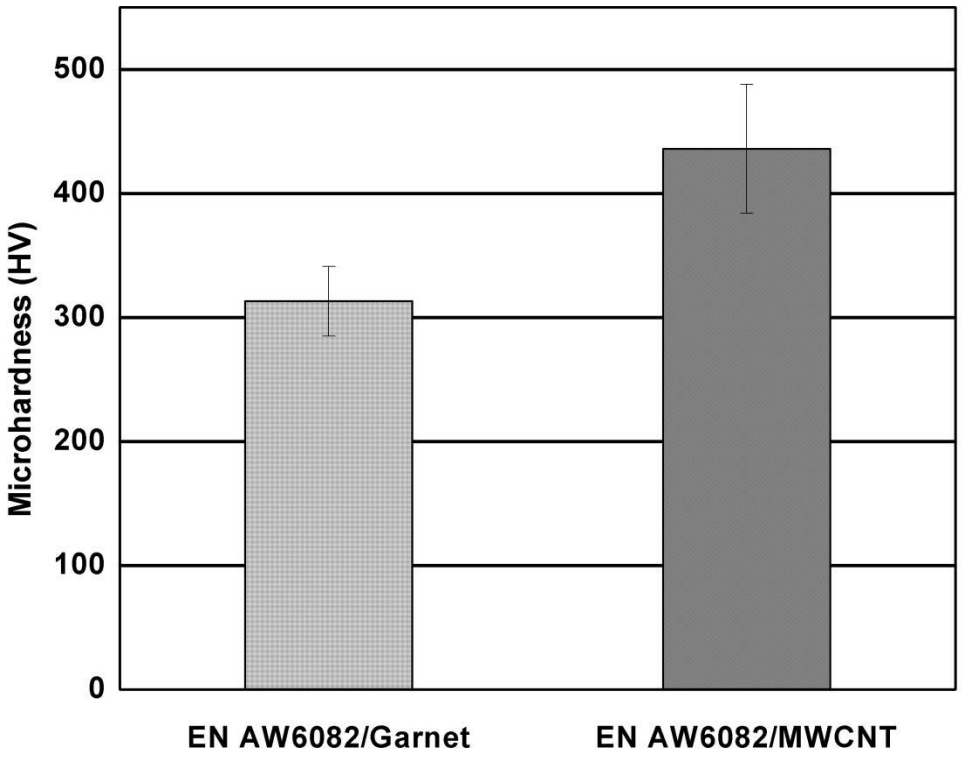

Figure 4.17: Microhardness of EN AW6082/Garnet and EN AW6082/MWCNT composite powders.

since the rigidity of MWCNT reinforcement is much higher than that of garnet. If modulus of the composite is higher hardness can also be expected to be higher (Ref 34). The above factors increases the strength of the matrix, and thus to the composite. The hardness values obtained are higher compared with initial hardness data of pure aluminum, aluminum alloy and composites milled for various milling time up to 50 h [Eskandarany (2001), Choi *et al.* (2001) and Mondolfo (1976)]. Fig. 4.18 shows a representative load vs. displacement curve, obtained using nanoindentation, for each composite. It shows that the depth of indent for EN AW6082/Garnet composite is 970 nm compared to 823 nm for EN AW6082/MWNCT. This indicates that the milled

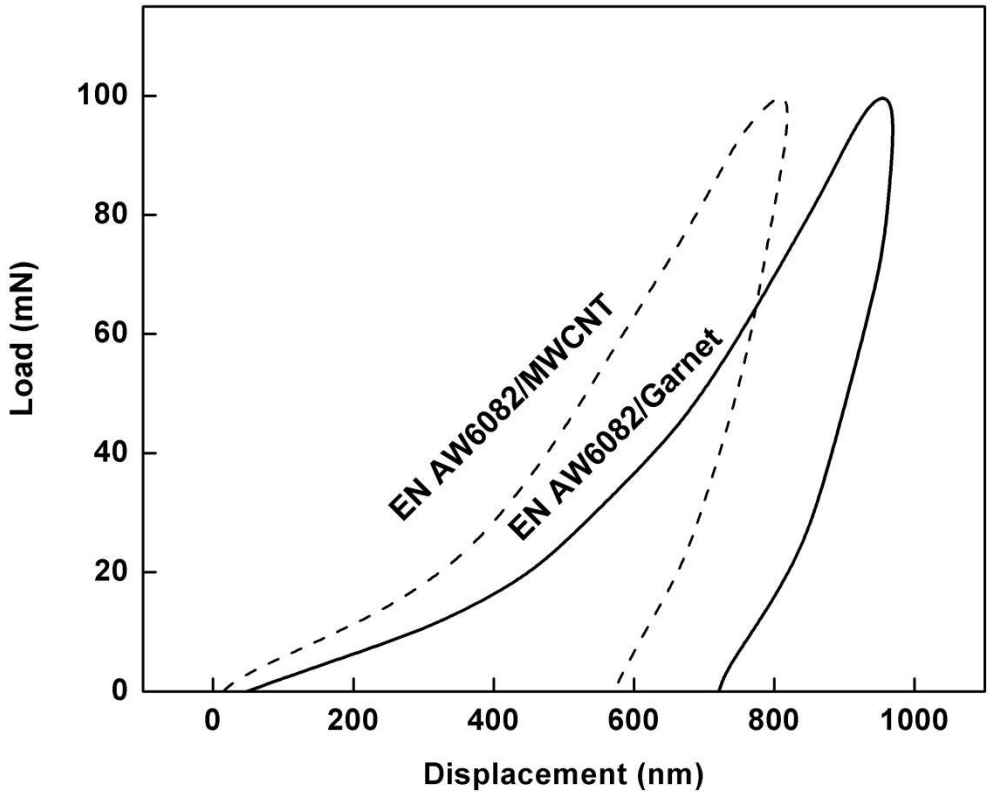

Figure 4.18: Load vs. displacement curves for garnet and MWCNT as reinforcement.

deformation is easiest in the case of EN AW6082/Garnet composite. Indentation depth is the measurement of elastic and plastic deformation together. Hence, the difficulty in deformation is actually the cumulative result of enhancement in elastic and plastic strengthening of the composite powders. It is clear from the depth of indentation that MWCNT addition strengthens the composite. The slope of the unloading curve is the measure of elastic modulus in nanoindentation measurements. From Fig. 4.18, it can be clearly noticed that EN AW6082/Garnet has the smaller unloading slope compared to

Table 4.3: Nanohardness and elastic modulus of composite constituents milled for 50h.

System	H(Gpa)	E (Gpa)
EN AW6082/Garnet	4.24 ± 0.07	148 ± 7
EN AW6082/MWCNT	5.90 ± 0.2	203 ± 9

EN AW6082/MWCNT. Nanohardness values and elastic modulus for mechanically composites, evaluated through nanoindentation technique, are given in Table 4.3. EN AW6082/MWCNT composite has the higher elastic modulus of 203 GPa compared to 148 GPa for EN AW6082/Garnet composite powders. Therefore, MWCNT reinforced alloy shows 1.3 and 1.4 times increase in modulus and hardness, respectively, compared to garnet reinforced composites. This is attributed to the homogenous dispersion of CNTs in the matrix. The reason for this difference can be due to good interfacial bonding between Al matrix and CNT, uniform distribution of CNTs in the Al-alloy matrix and thermal mismatch.

4.7 Conclusions

In the present investigation, EN AW6082 Al-alloy was successfully reinforced by the dispersion of 2 wt.% MWCNTs through high-energy ball milling and the ensuing powders were thoroughly characterized. Further effort was made to compare the MWCNT reinforced composite with that of garnet reinforced composite discussed in chapter 3. The following conclusions could be drawn from the present study:

(1) The reinforced composite powders showed a drastic crystallite size refinement from 165 nm at 10 h to about 28 nm after 50 h milling in presence of MWCNT. This has been ascribed to the impediment of the movement of the dislocation by Orowan strengthening and embedment of CNT at grain boundaries. The

morphological studies showed that the CNT's were shortened to a greater extent and got homogenously dispersed and embedded in the soft Al matrix. The TEM study corroborated the presence of nanoscale CNTs in Al matrix.

(2) The presence of nanoscale CNTs led to a two fold increase in the hardness and modulus of EN AW6082 alloy. The microhardness and nanohardness of the composites displayed significant increase for the composite reinforced with 2 wt.% MWCNT over the unreinforced EN AW6082 alloy produced by the same route. The hardness reaches a maximum of 436 ± 52 HV after 50 h of milling.

(3) Aluminum matrix shows a reduction in crystallite size when reinforced with garnet and MWCNTs and milled for 50 h. The incorporation of MWCNTs give rise to a better grain size refinement compared to that obtained with garnet reinforcement. This is due to its effective combination of both ductile and brittle nature and nanoscale sized uniform dispersion in the matrix.

(4) Morphological studies on EN AW6082/MWCNT powders revealed that CNTs were densely packed by Al-matrix without any structural damage and got homogenously dispersed in the soft Al-alloy matrix.

(5) Hardness and elastic modulus of MWCNTs reinforced powders are higher than that of garnet reinforced composites. This is attributed to homogenous dispersion of CNTs and good interfacial bonding between Al-alloy matrix and CNT.

(6) It can be concluded from the present study that MWCNTs is a better reinforcing candidate for EN AW6082 compared to garnet. However, garnet being an industrial by-product shows potential for improved properties than that of unreinforced Al-alloy and hence forms an excellent choice as reinforcement from waste utilization view points.